ISSN 1070-3284, Russian Journal of Coordination Chemistry, 2019, Vol. 45, No. 4, pp. 273–287. © Pleiades Publishing, Ltd., 2019.
Russian Text © S.A. Nikolaevskii, M.A. Kiskin, A.G. Starikov, N.N. Efimov, A.S. Bogomyakov, V.V. Minin, E.A. Ugolkova, O.M. Nikitin, T.V. Magdesieva, A.A. Sidorov, I.L. Eremenko, 2019, published in Koordinatsionnaya Khimiya, 2019, Vol. 45, No. 4, pp. 219–234.

Dedicated to the 90th birthday of Academician I.I. Moiseev

Atmospheric Oxygen Influence on the Chemical Transformations of 4,5-Dimethyl-1,2-Phenylenediamine in the Reactions with Copper(II) Pivalate

S. A. Nikolaevskii[a], *, M. A. Kiskin[a], A. G. Starikov[b], N. N. Efimov[a], A. S. Bogomyakov[c], V. V. Minin[a], E. A. Ugolkova[a], O. M. Nikitin[d], T. V. Magdesieva[d], A. A. Sidorov[a], and I. L. Eremenko[a]

[a] *Kurnakov Institute of General and Inorganic Chemistry, Russian Academy of Sciences, Moscow, 119991 Russia*
[b] *Institute of Physical and Organic Chemistry, Southern Federal University, Rostov-on-Don, Russia*
[c] *International Tomography Center, Siberian Branch, Russian Academy of Sciences, Novosibirsk, Russia*
[d] *Faculty of Chemistry, Moscow State University, Moscow, Russia*
**e-mail: sanikol@igic.ras.ru*

Received November 9, 2018; revised November 26, 2018; accepted November 27, 2018

Abstract—The one-pot synthesis of the Cu(II) complex with hard to access symmetric bis-azoligand is carried out by the reaction of 4,5-dimethyl-1,2-phenylenediamine (Dmpda) with the $[Cu_2(Piv)_4(HPiv)_2]$ complex (Piv is the pivalate anion) in the presence of atmospheric oxygen. The amine form of the ligand takes place and the bis-diiminosemiquinone biradical redox form of the ligand does not take place in the $[CuL^{azo}]$ complex as unambiguously shown by the data of X-ray structure analysis (CIF files CCDC nos. 1877582 (**I** · DMF) and 1877583 (**II**), ESR spectroscopy, SQUID magnetometry, and electrochemical and quantum chemical studies. The coordination polymer $[Cu_2(Piv)_4(Dmpda)]_n$ in which the Dmpda molecules perform the bridging function is formed in the same reaction mixture under reduced air pressure.

Keywords: redox-active ligands, carboxylate complexes, synthesis, structure, reactivity

DOI: 10.1134/S1070328419040067

INTRODUCTION

It is known that *ortho*-phenylenediamines as ligands coordinating with metal centers behave in different manners depending on the positions of the amino groups in the aromatic ring, hydrocarbon substituents in the phenylene core, and geometric and electronic characteristics of the metal ion to which binding occurs. These processes can give various architectures of complexes from mononuclear products to coordination polymers [1–10]. For example, ions of the nickel subgroup (Ni(II), Pd(II), and Pt(II)) reacting with *ortho*-phenylenediamine and its substituted derivatives in an air atmosphere stimulate the oxidative dehydrogenation of the diimine ligand to form the mononuclear bis-*ortho*-semiquinonediimine complexes in which the metal ions exist in the planar-square environment [3, 11–13]. At the same time, the oxidation process can be continued using the silver salts, which leads to the dimeric cations $[M(1,2\text{-}(NH)(NR)C_6H_4)_2]^{2+}$ (M = Ni(II), Pd(II), and Pt(II)) with a weak metal–metal bond [2, 5, 14].

Similar reactions with Co(II) pivalate in air are accompanied by the formation of semiquinonediimine ligands and also by the oxidation of the cobalt ion to the trivalent state in the $[Co\{\eta^2\text{-}(NPh)(NH)C_6H_4\}_2\{\eta^1\text{-}(NH_2)C_6H_4(NPhH)\}]^+$ cation [15]. Note that this complex contains both oxidized and nonoxidized molecules of substituted *ortho*-phenylenediamine. It is most likely that the possibility of diamine oxidation is determined by the electrochemical potential of the metal center in which the organic ligand is transformed after its coordination and by the reaction medium, which undoubtedly includes the atmosphere where the reactions occur (air, gas-oxidant (for example, CO_2), inert gas, etc.). For example, when nickel pivalate is used in this process, an intermediate complex $[Ni(\eta^2\text{-}o\text{-}(NH_2)_2C_6H_4)_2](Piv)_2$ with two molecules of nonoxidized diamine coordinated via the chelating mode, which is transformed in an air atmosphere into the bis(semiquinonediimine) monomer $[Ni(1,2\text{-}(NH)(NPh)C_6H_4)_2]$ with the Ni(II) ion. No further oxidation occurs under aerobic conditions. At the

same time, in a diamine excess the ligand molecules are oxidized and also become bridging in the trinuclear $[Ni_3\{\mu\text{-}N,N'\text{-}(NH_2)_2C_6H_4\}_2(HPiv)_3(\mu_3\text{-}OH)(\mu\text{-}Piv)_4]^+$ cation [16]. When forming complexes with *d*-metal ions, similar aromatic diamines can be transformed into various species and can form fairly unusual organic moieties, and unique organic molecules unbound to the metal ions can also be generated in some cases. For example, when the platinum or nickel bis(chelate) complexes with *N*-phenyl-*o*-benzosemiquinonediimine are oxidized with a silver trifluoromethanesulfonate excess in an acetone solution, the complex slowly decomposes to form the heterocyclic condensation product of two ligands of the "head-to-tail" type containing no metal atoms, as well as two peripheral nitrogen atoms are condensed with the acetone molecule to form the imidazole fragment (Scheme 1).

The condensation of amines with aldehydes and ketones affords, as a rule, the corresponding Schiff bases. However, in the presence of air oxygen coordinated 4,5-dimethyl-1,2-phenylenediamine (Dmpda) reacts with phthalaldehyde to form 4,5-dimethyldiisoindolo[2,1-*a*:1,2-*c*]quinoxaline-1,8-dione [17]. Note that this reaction does not occur without Ni(II) ions as in the case of the replacement of the nickel derivatives by compounds with other divalent *d*-metal ions [18].

(a) (b)

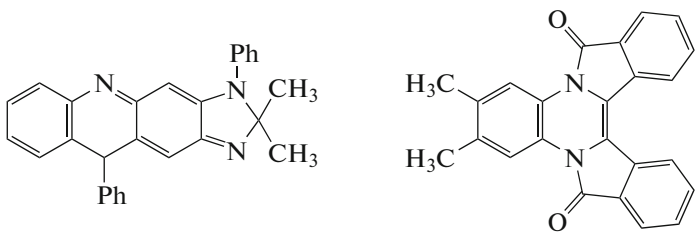

Molecules of (a) 2,2-dimethyl-1-phenyl-3-imidazo[4,5-*b*]-5-phenyl-1,2-dihydrophenazine and (b) 4,5-dimethyldiisoindolo[2,1-*a*:1,2-*c*]quinoxaline-1,8-dione

Scheme 1.

As follows from the above examples (their number is really much higher), it seems possible to control the formation of new ligands from *ortho*-phenylenediamines bound to the metal centers by the variation of the reaction conditions and, in particular, the composition of the gas atmosphere in which the reactions occur.

The results of studying the reaction of copper(II) pivalate $[Cu_2(\mu\text{-}Piv)_4(HPiv)_2]$ with Dmpda in air and under reduced pressure due to the evacuation (water-jet pump) of the starting reaction solution in toluene are presented in this work.

EXPERIMENTAL

Commercially available solvents and Dmpda (98%, Sigma Aldrich) were used as received. Copper(II) pivalate $[Cu_2(Piv)_4(HPiv)_2]$ was synthesized according to the described procedure [19, 20].

Synthesis of $[CuL^{azo}]$ (I). Solid Dmpda (0.1634 g, 0.0012 mol) was added to a solution of $[Cu_2(Piv)_4(HPiv)_2]$ (0.1472 g, 0.0002 mol) in benzene (30 mL) at 60°C. The color of the reaction mixture changed from blue to black. The reaction mixture was kept at this temperature with vigorous stirring for 3 h, then cooled to room temperature, and left overnight. The formed brown precipitate was filtered off and washed with ethanol to a colorless filtrate. The brown powder was extracted with chloroform (15 mL). The extract obtained was dried in air to a constant weight. The yield of $[CuL^{azo}]$ was 0.1220 g (66% based on the starting amount of Dmpda).

For $C_{24}H_{26}N_6Cu$			
Anal. calcd., %	C, 62.39	H, 5.67	N, 18.19
Found, %	C, 62.20	H, 5.58	N, 18.27 (for powder obtained from synthesis)

IR (ATR; ν, cm^{-1}): 3304 s, 3289 s, 2908 m, 1663 vs, 1630 vs, 1523 s, 1485 vs, 1444 vs, 1406 m, 1376 s, 1335 vs, 1299 vs, 1275 vs, 1234 vs, 1177 s, 1154 vs, 1086 vs, 1025 vs, 1004 vs, 880 vs, 870 vs, 852 vs, 787 s, 734 s, 721 vs, 658 vs, 611 s, 565 m, 522 s, 488 vs, 453 s, 431 m, 411 m.

A minor amount of the obtained powder was dissolved in dimethylformamide (DMF) and left in an open conic flask at room temperature. Black crystals formed in two weeks suitable for X-ray structure analysis were separated from the mother liquor, washed with diethyl ether, and dried in air.

Synthesis of $[Cu_2(Piv)_4(Dmpda)]_n$ (II). A solution of Dmpda (0.0681 g, 0.0005 mol) in toluene (15 mL)

was added to a solution of $[Cu_2(Piv)_4(HPiv)_2]$ (0.3679 g, 0.0005 mol) in toluene (15 mL) at room temperature. The Schlenk flask with the formed solution was evacuated for 15–20 s using a water-jet pump to remove air. The solution was left to stay under low vacuum. A blue-green precipitate was formed within 5–7 min. The reaction mixture with the precipitate was kept for 2 days in the Schlenk flask at room temperature. The precipitate formed was filtered off, washed with toluene (15 mL), and dried in air to a constant weight. The yield of compound **II** was 0.1745 g (46% taking into account the solvate toluene molecule).

Single crystals of **II** · C_7H_8 suitable for X-ray structure analysis were obtained by slow mixing of dilute toluene solutions of the starting compounds. The IR spectra of the single crystals and polycrystalline product were completely identical. The correspondence of the structures of the single crystals and polycrystalline phase was unambiguously established by powder X-ray diffraction.

For $C_{35}H_{56}N_2O_8Cu_2$ (**II** · C_7H_8)

Anal. calcd., %	C, 55.32	H, 7.43	N, 3.69
Found, %	C, 55.03	H, 7.69	N, 3.56

IR (ATR; ν, cm^{-1}): 3371 w, 3284 w, 2957 m, 2926 m, 2867 m, 1621 s, 1597 vs, 1519 s, 1481 vs, 1457 m, 1416 vs, 1376 s, 1360 s, 1297 m, 1224 vs, 1200 m, 961 s, 927 s, 896 s, 848 m, 824 w, 800 m, 788 s, 740 w, 716 m, 691 m, 619 vs, 573 w, 482 m, 460 s, 442 vs.

The X-ray structure analyses of the single crystals of complexes **I** · DMF and **II** were carried out on a Bruker Apex II diffractometer (CCD detector, MoK_α, λ = 0.71073 Å, graphite monochromator) [21]. A semiempirical absorption correction was applied [22]. The structures were solved by direct methods and refined anisotropically in the full-matrix approximation for all non-hydrogen atoms. The hydrogen atoms at the carbon atoms of the organic ligands were generated geometrically and refined by the riding model. The calculations were performed using the SHELX-97 program package [23]. The crystallographic parameters and structure refinement details for compounds **I** · DMF and **II** are presented in Table 1. Selected bond lengths and bond angles are given in Table 2.

The coordinates of atoms and other parameters of the structures were deposited with the Cambridge Crystallographic Data Centre (CIF files CCDC nos. 1877582 (**I** · DMF) and 1877583 (**II**); deposit@ccdc.cam.ac.uk or http://www.ccdc.cam.ac.uk/data_request/cif).

The magnetic properties of a polycrystalline sample of compound **I** were studied on an MPMS-XL SQUID magnetometer (Quantum Design) in a temperature range of 2–300 K in a magnetic field of 5 kOe. Diamagnetic corrections were applied according to Pascal's additive scheme [24] to calculate the paramagnetic component of the molar magnetic susceptibility (χ).

The magnetic properties of a polycrystalline sample of compound **II** were measured using the PPMS-9 Quantum Design automated complex for measuring physical properties. The temperature dependences of the magnetization were measured in a temperature range of 2–300 K in the external magnetic field with the intensity H = 5 kOe. Corrections to the magnetic properties of the sample holder and diamagnetism of the compound were applied using Pascal's scheme [24].

The effective magnetic moment (μ_{eff}) was determined in the paramagnetic range using the equation $\mu_{eff} = \left(\frac{3k}{N_A\beta^2}\chi T\right)^{1/2} \approx (8\chi T)^{1/2}$, where k is the Boltzmann constant, N_A is Avogadro's number, and β is Bohr magneton.

ESR spectra were recorded on a Bruker ELEXSYS E-680X instrument in the X range at T = 293 K.

Quantum chemical calculations were performed using the Gaussian 09 program [25] by the density functional theory (DFT) in the B3LYP/6-311++G(d,p) approximation, which correctly reproduced the geometric and energetic characteristics of the transition metal complexes [26]. Stationary points were localized on the potential energy surface using the full geometry optimization of the molecular structures and checking the DFT wave function stability. The graphical images illustrating the calculation results were obtained using the ChemCraft program [27].

Electrochemical studies were carried out in preliminarily prepared solvents. Dimethylformamide (high-purity grade) was distilled in vacuo (12 mmHg) over P_2O_5 collecting the fraction with bp = 45–46°C. Acetonitrile (Aldrich, HPLC grade) was distilled over P_2O_5 collecting the fraction with bp = 81–82°C (760 mmHg).

The electrochemical oxidation and reduction potentials were measured on an AutoLab PGSTAT100N potentiostat. Voltammograms were recorded against 0.05 M n-Bu_4NBF_4 in DMF at 20°C in an 8-mL electrochemical cell. Oxygen was removed from the cell by purging dry argon. Voltammetric curves were detected by cyclic voltammetry (CV) on a stationary platinum electrode at different potential sweeps. A Pt wire served as an auxiliary electrode. A saturated silver chloride electrode with a potential of −0.53 V (vs. Fc/Fc^+ in DMF) was used as a reference electrode. The measured values of potentials were recalculated taking into account ohmic losses.

A Vulcan graphite powder (10 mg) was mixed with dodecyl(tri-*tert*-butyl)phosphonyl tetrafluorob-

Table 1. Crystallographic data and calculated parameters for the structures of the crystals of $[CuL^{azo}] \cdot DMF$ and $[Cu_2(Piv)_4(Dmpda)]_n$

Parameter	Value	
	$[CuL^{azo}] \cdot DMF$	$[Cu_2(Piv)_4(Dmpda)]_n$
Empirical formula	$C_{27}H_{33}N_7OCu$	$C_{35}H_{56}N_2O_8Cu_2$
FW	535.14	1471.10
T, K	150(2)	173(2)
Crystal system	Triclinic	Monoclinic
Space group	$P\bar{1}$	$C2/c$
a, Å	9.1615(7)	11.3766(14)
b, Å	10.4948(8)	24.030(3)
c, Å	14.0821(11)	15.2038(19)
α, deg	96.502(2)	90.00
β, deg	100.501(2)	98.927(2)
γ, deg	105.7690(10)	90.00
V, Å^3	1262.09(17)	4106.0(9)
Z	2	4
ρ_{calcd}, g cm^{-3}	1.408	1.229
μ, mm^{-1}	0.900	1.081
Crystal size, mm	0.05 × 0.03 × 0.02	0.43 × 0.13 × 0.07
θ_{min}–θ_{max}, deg	1.49–28.28	1.69–27.68
F(000)	562	1608
T_{min}/T_{max}	0.9564/0.9822	0.6304
Ranges of reflection indices	$-11 \le h \le 12$, $-13 \le k \le 13$, $-18 \le l \le 18$	$-14 \le h \le 14$, $-31 \le k \le 31$, $-19 \le l \le 19$
Measured reflections	12447	20311
Independent reflections (R_{int})	6151 (0.0564)	4818 (0.9282)
Reflections with $I > 2\sigma(I)$	4038	3218
GOOF	1.057	1.001
R factors for $F^2 > 2\sigma(F^2)$	$R_1 = 0.0536$, $wR_2 = 0.1055$	$R_1 = 0.0523$, $wR_2 = 0.1312$
R factors for all reflections	$R_1 = 0.0968$, $wR_2 = 0.1338$	$R_1 = 0.0923$, $wR_2 = 0.1582$
Residual electron density (min/max), e/Å^3	−0.523/0.468	−1.041/0.593

orate (10 mg) in an garnet mortar to prepare a carbon paste. The components were thoroughly stirred to a homogeneous paste, electrochemically active substance **II** (6 mg) was added to the paste, and the mixture was again stirred thoroughly and collected in a Teflon tube 1.5 mm in diameter. The carbon paste in the tube was packed with a copper wire, and the latter was left in the tube. The obtained paste carbon electrode was immersed into a supporting electrolyte solution (0.15 M Bu_4NBF_4, CH_3CN) in the electrochemical cell and used as the working electrode.

RESULTS AND DISCUSSION

As expected, the reaction of Dmpda with copper(II) pivalate in toluene in the presence of air oxygen resulted in the oxidative dehydrogenation of the ligand. However, an unusual process is observed in the case of the copper complex: dehydrogenation accompanied by the condensation of three diamine molecules leading to the formation of the 4,5-dimethyl-1,2-phenylenebis(diazo-1,2-diyl)bis(3,4-dimethylaniline) ligand (H_2L^{azo}) chelating the Cu(II) ion in the new $[CuL^{azo}]$ complex (Scheme 2).

Table 2. Selected bond lengths and angles in complex **I** · DMF

Bond	Å	Bond	Å
Cu(1)–N(1)	1.903(3)	Cu(1)–N(3)	1.952(3)
Cu(1)–N(4)	1.945(3)	Cu(1)–N(6)	1.905(3)
C(1)–C(2)	1.420(5)	C(17)–C(22)	1.441(5)
C(1)–C(6)	1.441(5)	C(18)–C(19)	1.356(5)
C(2)–C(3)	1.377(4)	C(19–C(20)	1.428(5)
C(3)–C(4)	1.435(5)	C(20)–C(21)	1.372(4)
C(4)–C(5)	1.357(5)	C(21)–C(22)	1.432(4)
C(5)–C(6)	1.427(4)	N(1)–C(22)	1.330(4)
C(9)–C(10)	1.393(4)	N(2)–C(17)	1.358(4)
C(9)–C(14)	1.410(4)	N(3)–C(14)	1.411(4)
C(10)–C(11)	1.382(5)	N(4)–C(9)	1.414(4)
C(11)–C(12)	1.420(5)	N(5)–C(6)	1.354(4)
C(12)–C(13)	1.384(4)	N(6)–C(1)	1.334(4)
C(13)–C(14)	1.386(4)	N(2)–N(3)	1.305(4)
C(17)–C(18)	1.425(4)	N(4)–N(5)	1.300(3)
Angle	ω, deg	Angle	ω, deg
N(1)Cu(1)N(3)	90.46(11)	N(4)Cu(1)N(3)	83.71(11)
N(1)Cu(1)N(4)	173.88(12)	N(6)Cu(1)N(3)	172.03(12)
N(1)Cu(1)N(6)	95.47(12)	N(6)Cu(1)N(4)	90.16(11)

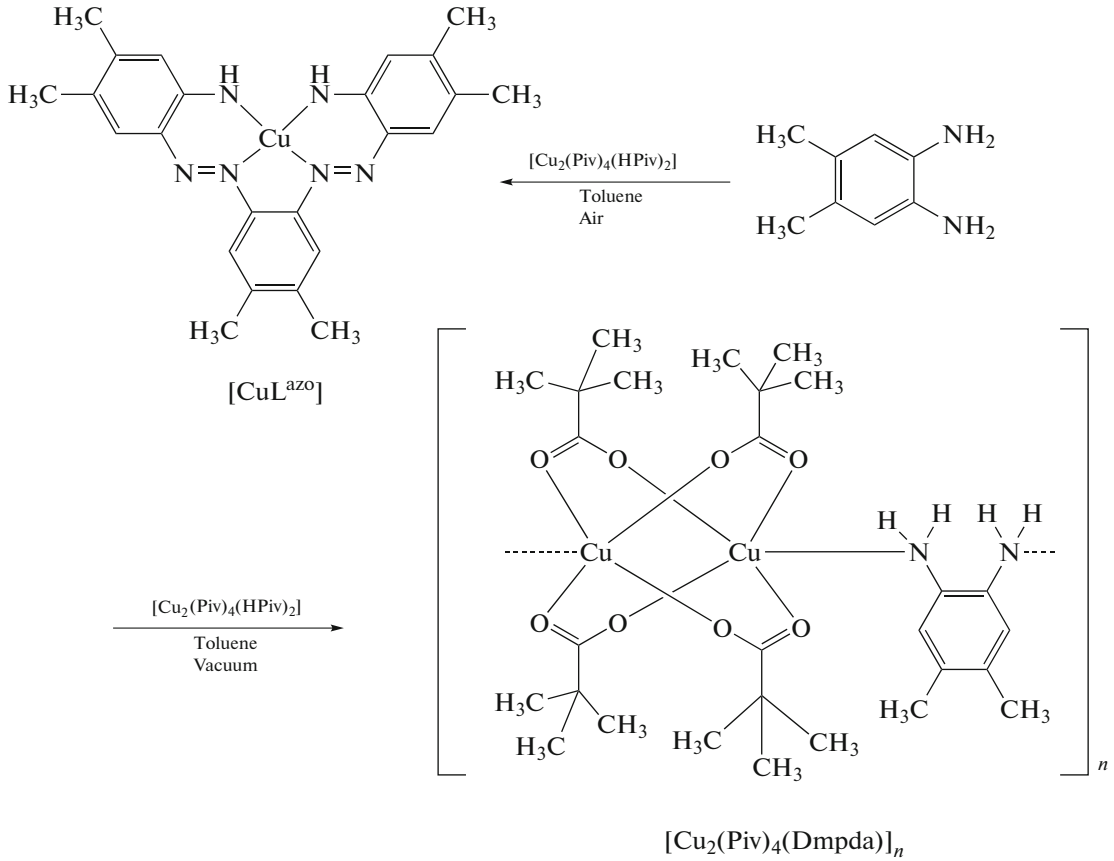

Reactivity of Dmpda toward complex $[Cu_2(Piv)_4(HPiv)_2]$

Scheme 2.

Note that the synthesis of organic diazo compounds of a similar type is a nontrivial task [28–30] and is of independent scientific interest, since these compounds are precursors of azobenzophanes, which represent a promising class of (chiro)optical switches [28, 31–35]. For example, it was shown [28] that similar diaminobisazobenzenes can be synthesized from *o*-phenylenediamine using multistage schemes only.

We obtained different results when this reaction was carried out in toluene with the preliminary evacuation of the reaction solution for 15–20 s (we didn't measure real residual pressure in the Schlenk reaction vessel) to remove possible oxidants (O_2, CO_2) from the reaction atmosphere. In this case, no oxidative dehydrogenation occurs and coordination polymer **II** is formed in which the starting diamine performed the bridging function binding the binuclear tetrapivalate metal fragments with the copper(II) atoms to form the chain 1D architecture.

The structure of compound **I** · DMF is presented in Fig. 1. The doubly deprotonated molecule of 4,5-dimethyl-1,2-phenylenebis(diazo-1,2-diyl)bis(3,4-dimethylaniline) acting as a tetradentate ligand closes one five- and two six-membered rings by the copper atom. The central metal atom exists in a distorted planar-square environment of four nitrogen atoms (the Cu(1) atom shifts from the N(1)N(3)N(4)N(6) plane by 0.062(2) Å). The main bond lengths and bond angles are presented in Table 2. An analysis of the crystal packing of complex **I** · DMF showed the formation of a hydrogen bond between the H(1A) atom and the O atom of the solvate DMF molecule: (N(1)···O(1S) 3.038, H(1A)···O(1S) 2.20 Å, angle N(1)–H···O(1S) 159.1° (Fig. 1a). Intermolecular interactions between two molecules of the complex (Cu(1)···C(12*A*) 3.324(4), C(13)···N(4*A*) 3.467(5) Å; index symmetry: (*A*) $-x-2, -y-2, -z$) were also revealed resulting in a supramolecular dimer with the Cu(1)···Cu(1*A*) distance equal to 5.8207(7) Å (Fig. 1b).

The most interesting structural feature of complex **I** · DMF is the presence of two pairs of C(2)–C(3), C(4)–C(5) and C(18)–C(19), C(20)–C(21) bonds, which are noticeably shortened over the characteristic values of aromatic C–C bonds [36]. An analysis of the published data [37–45] shows that a similar alternation of bonds is typical of the azo complexes of copper and other transition metals [46]. It is concluded [45] on the basis of the X-ray structure data for the mononuclear copper(II) complex with the 2,2'-dihydroxyazobenzene derivative and pyridine that the observed bond alternation is caused by the conjugation of the aromatic rings with the azo group, which induces the electron density redistribution in the whole molecule. The distribution of the bond lengths N(2)–C(17), N(2)–N(3), and N(3)–C(14) (N(5)–C(6), N(4)–N(5), and N(4)–C(9)) observed in compound **I** · DMF is consistent with the published data [45, 46]. The formation of the benzosemiquinonediimine form of the ligand, which is produced by the oxidation of *ortho*-phenylenediamines in the reactions of *d*-metal salts, cannot formally be excluded for compound **I** · DMF, because the electron density redistribution in the formed metallocycles should also be observed in this case [13].

Although the probability for the possible electromer [$CuL^{azo\text{-}ibsq}$] (**Ia**) to exist seems rather low, the X-ray structure analysis data formally did not expel its formation in this structure (Scheme 3). Taking into account the results [47] indicating that the structural criterion should be used carefully for the identification of the electronic structures of the redox-active ligands, we performed the quantum chemical study in order to elucidate reasons for unusual geometric characteristics of [CuL^{azo}].

(a) (b)

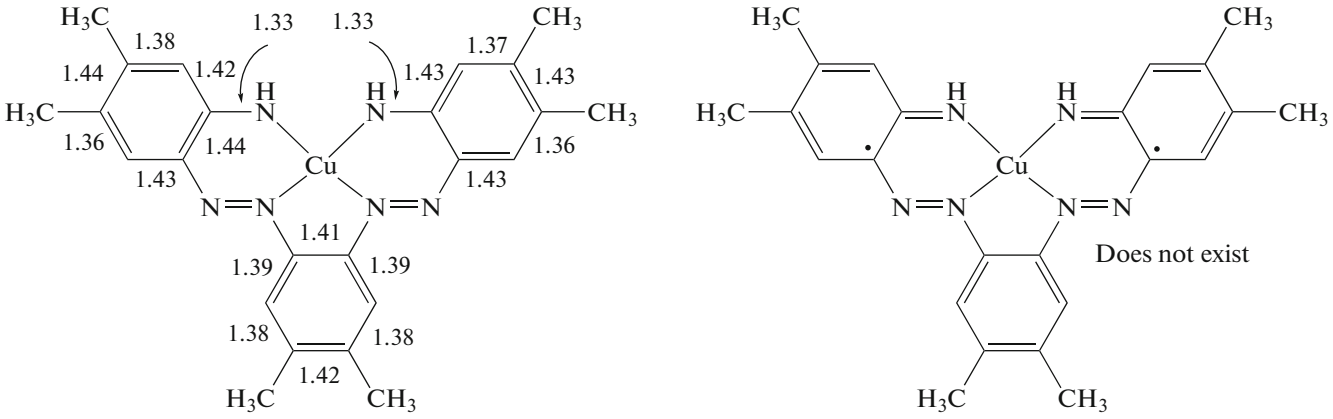

(a) Bond lengths in complex **I** · DMF and (b) hypothetical structure of electromer [$CuL^{azo\text{-}ibsq}$]

Scheme 3.

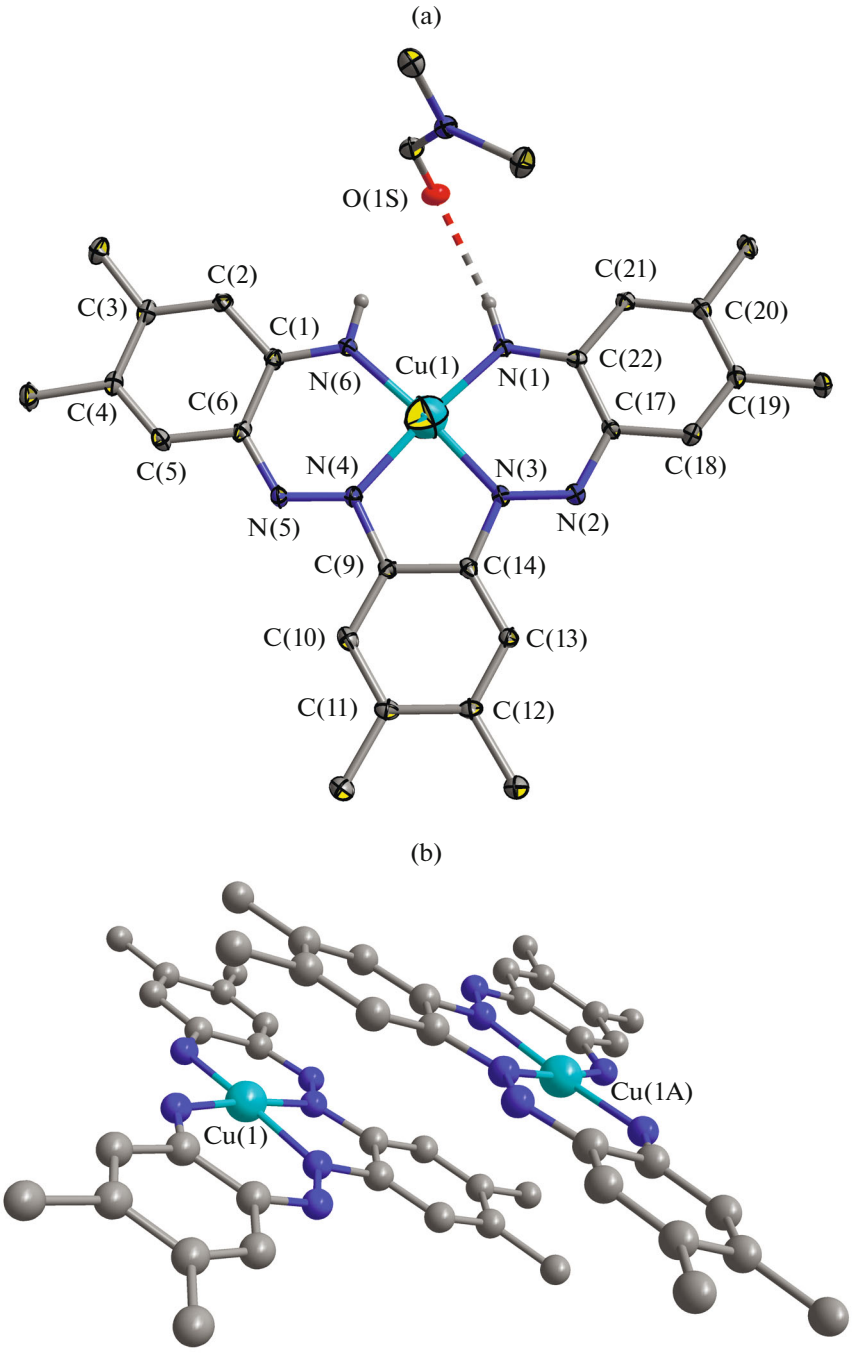

Fig. 1. (a) Molecular structure and (b) packing fragment of molecules of complex **I** · DMF in crystal; (a) thermal ellipsoids with 30% probability; hydrogen atoms are omitted.

As shown by the calculation results, the optimized geometry of complex **I** is well consistent with the X-ray structure analysis data (Fig. 2a). The search for an electromer containing two unpaired electrons on the ligand gave the structure (Fig. 2b) destabilized by more than 33 kcal/mol over the ground state. The calculated difference in energies indicates that this state of the complex cannot exist.

The spin density distribution found in a molecule of compound **I** indicates the localization of a significant fraction of the spin density on the metal (0.49). This value is lower than those observed in the mononuclear copper chelates. Model structures **III** and **IV** were calculated to explain the obtained result.

As follows from the spin density distribution presented in Fig. 3, the main reason for a reduced value of

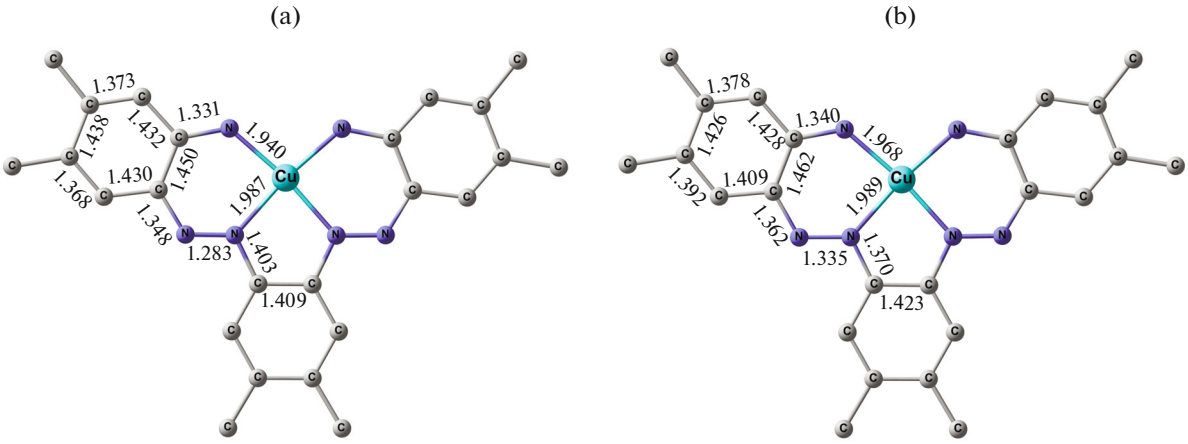

Fig. 2. Optimized geometries of (a) complex **I** and (b) electromer **Ia** calculated by the B3LYP/6-311++G(d,p) method.

the spin density on the copper atom is the nitrogen atom not bound to the metal atom, which draws off some spin density. The replacement of this atom (nitrogen) by the CH group leads to the value typical of the copper complexes: 0.57. Thus, the calculation results show that the benzosemiquinonediimine form of complex **Ia** is not observed and the bond length distribution unusual for aromatic systems is due to the presence of the azo group.

Compound **II** is a coordination 1D polymer in which the tetracarboxylate fragments $\{Cu_2(Piv)_4\}$ are linked into a chain by the bridging Dmpda molecules (Fig. 4).

The C(11)–C(12) and C(12)–C(13) bonds are shortened insignificantly (0.01–0.02 Å), the C(11)–N(1) bond is elongated by 0.04 Å, and the C(13)–C(14) bond length undergoes no changes compared to similar values in the initial Dmpda molecule [48, 49]. The geometry of the $\{Cu_2(Piv)_4\}$ fragment remains almost unchanged compared to that in the starting compound $[Cu_2(Piv)_4(HPiv)_2]$ [19]. Each copper atom exists in the environment of four oxygen atoms from four carboxylate groups. The coordination polyhedron of copper is supplemented to a distorted square pyramid by binding with the N(1) atom (Cu(1)–N(1) 2.226(3) Å) of the amino group. The O(1), O(2A), O(3A), and O(4) atoms lie in almost the same plane. The shift of the Cu(1) atom from this plane is 0.188(3) Å.

The ESR spectrum of a powder of compound **I** represents a nonsymmetric single line with an average g factor of 2.058 (Fig. 5a).

The ESR spectrum of compound **I** in a chloroform solution at room temperature (Fig. 5b) is described by the isotropic spin-Hamiltonian of the copper ion $S = 1/2$ with the Zeeman and hyperfine couplings with the nuclear spin of copper $I = 3/2$ and with an additional hyperfine coupling with the nuclear spins $I_a = 1$ of two pairs of equivalent nitrogen atoms

$$\hat{H} = g\beta HS + A^0 IS + g\beta\sum_{\alpha} a_{\alpha}^0 I_{\alpha} S, \qquad (1)$$

where g is the averaged component of the g tensor of the copper ion, A^0 is the averaged component of the hyperfine coupling structure (HFS) tensor of the copper ion expressed in cm^{-1}, a^0 is the averaged component of the additional hyperfine coupling structure (AHFS) tensor expressed in G, and $S = 1/2$.

The ESR spectral parameters were determined by the best fit method between the experimental and theoretical spectra using error functional minimization

$$F = \sum_i \left(Y_i^T - Y_i^E\right)^2 \Big/ N. \qquad (2)$$

Here Y_i^E is the set of experimental values of the ESR signal intensity with a constant increment over the magnetic field H, Y_i^T are the theoretical values at the same field intensities H, and N is the number of points. The theoretical spectra were constructed by the method described earlier [50]. The sum of the Lorentzian and Gaussian functions was used as a function of the line shape [51]. According to the relaxation theory [52], the line width was specified by the equation

$$\sigma = \alpha + \beta m_I + \gamma m_I^2, \qquad (3)$$

where m_I is the nuclear spin projection onto the magnetic field direction, and α, β, and γ are the broadening parameters. The g factor, HFS and AHFS constants, and line widths and shapes were varied in the course of minimization.

Thus, the ESR data completely confirm the theoretical calculations and conclusions about the absence

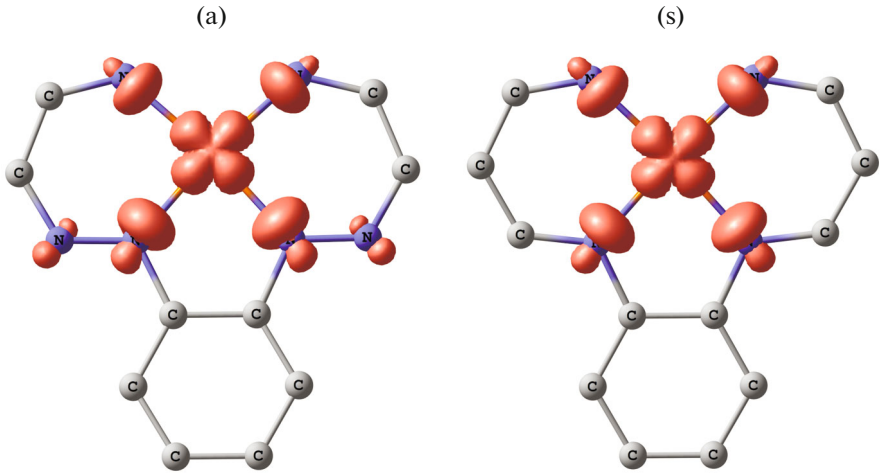

Fig. 3. Spin density distribution in model structures (a) **III** and (b) **IV**.

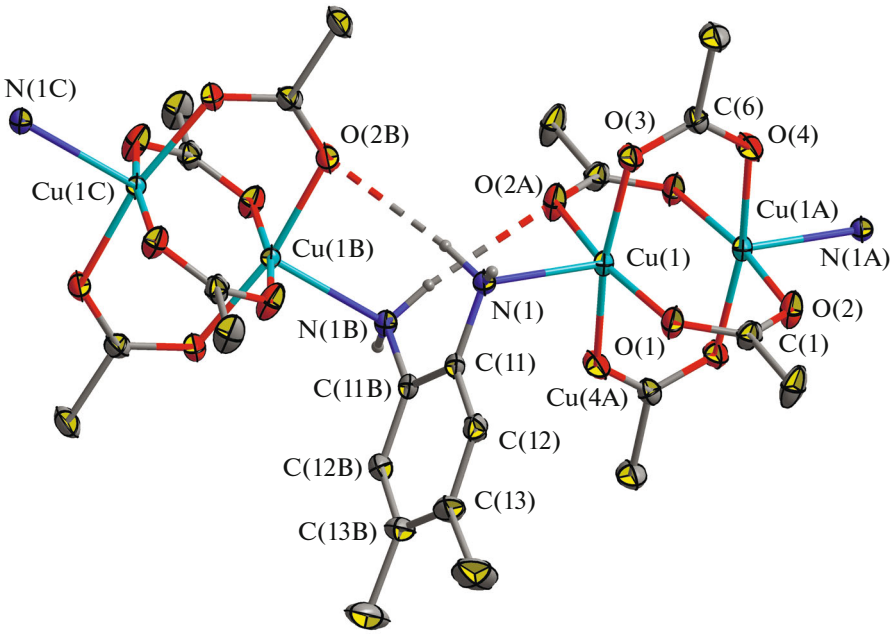

Fig. 4. Fragment of the polymer chain of complex **II** (thermal ellipsoids with 30% probability; hydrogen atoms at carbon atoms and methyl groups at *tert*-butyl groups are omitted).

in complex **I** of the benzosemiquinonediimine form of the ligand containing unpaired electrons.

The shape of the ESR spectrum of compound **II** (Fig. 6) is characteristic of the complex with the full spin $S = 1$ if the splitting value in the zero field D nearly coincides with the frequency $h\nu$. In the case considered, the spin-Hamiltonian takes the form

$$\hat{H} = g_{\perp}\beta(S_x H_x + S_y H_y) + g_z \beta H_z S_z + D\left(S_z^2 - \frac{1}{3}(S+1)S\right), \quad (4)$$

where $\hat{S} = \hat{S}_1 + \hat{S}_2$ is the operator of the full spin of the dimer $S = 1$; S_x, S_y, and S_z are the projections of the full

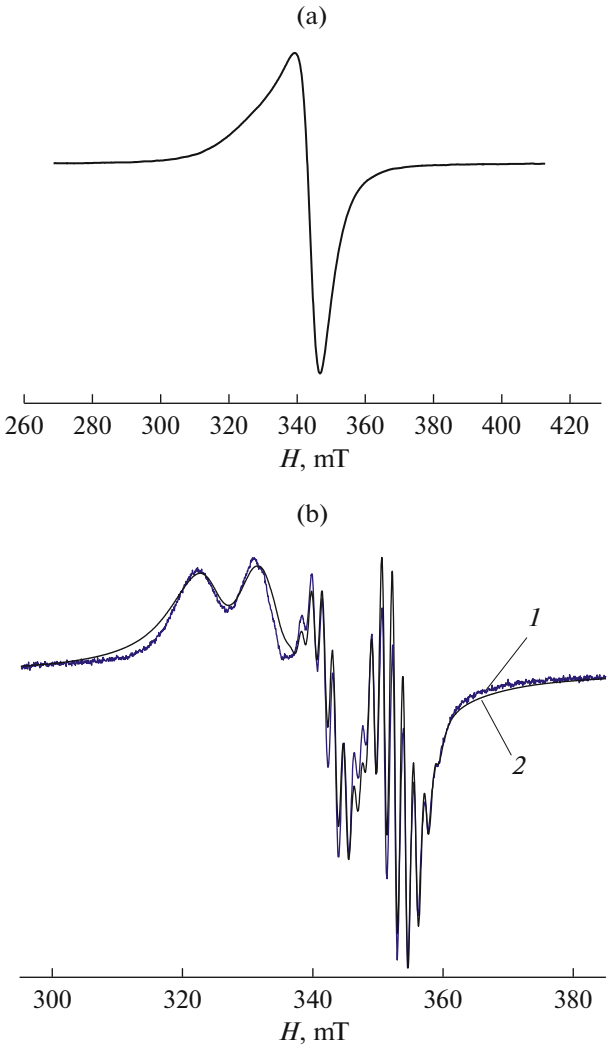

Fig. 5. ESR spectra of complex **I** as (a) a powder and (b) a solution in $CHCl_3$: (*1*) experimental and (*2*) theoretical spectra with the parameters of spin-Hamiltonian (1): g = 2.074, A^0(Cu) = 0.0086 cm^{-1}, $a^0(N1)$ = 15.971 G, and $a^0(N2)$ = 15.968 G.

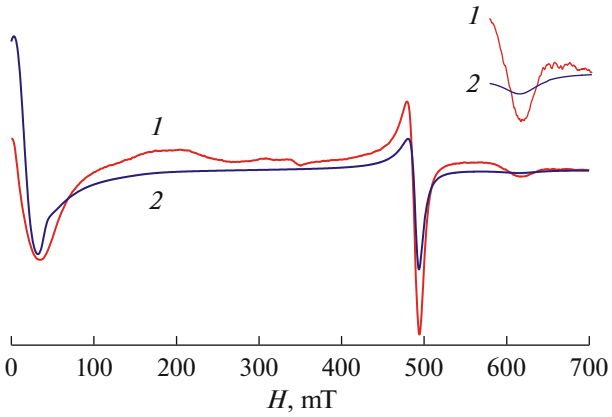

Fig. 6. ESR spectra of coordination polymer **II**: (*1*) experiment and (*2*) theory.

spin operator on the axes *x, y,* and *z*, respectively; D is the initial splitting (fine structure operator); and g_z and $g_\perp$ are the parallel and perpendicular components of the g tensor, respectively.

The numerical calculations of the resonance fields of spin-Hamiltonian (2) for the construction of the theoretical spectrum were performed using the Belford method [53].

The theoretical spectrum satisfactorily reproduces the experimental spectrum at the following parameters of spin-Hamiltonian (2): D = 0.3354 cm^{-1}, g_z = 2.31, and $g_\perp$ = 2.041.

The $\chi T(T)$ dependence for compound **I** is presented in Fig. 7a. At 300 K μ_{eff} (χT) = 1.99 μ_B (0.50 cm^3 K mol^{-1}), which is somewhat higher than the theoretical value equal to 1.73 μ_B (0.37 cm^3 K mol^{-1}) for one copper(II) ion (d^9, $^2D_{5/2}$, S = 1/2) with a g factor of 2. As the temperature decreases to 40 K, μ_{eff} remains almost unchanged, after which μ_{eff} decreases slightly to 1.42 μ_B (χT = 0.25 cm^3 K mol^{-1}) at 2 K. This probably indicates the appearance of weak intermolecular exchange interactions of the antiferromagnetic type between spins of the paramagnetic centers. According to the X-ray structure analysis data, the pairs of molecules with sufficiently short distances Cu(1)···Cu(1*A*) (5.821 Å) can be distinguished in the structure of compound **I** (Fig. 1b). Therefore, the model of exchange-coupled dimers (Hamiltonian $H = -2JS_1S_2$) was used for the analysis of the $\chi T(T)$ dependence. The optimum values of the g factor and exchange interaction parameter (***J***) are 2.06 (±0.01) and 0.98 (±0.02) cm^{-1}, respectively. The calculated g factor is consistent with the experimental one (2.058) determined by ESR spectroscopy for the solid sample.

The examination of the temperature dependence of the magnetic susceptibility of compound **II** in a range of 2–300 K revealed the magnetic interactions of the antiferromagnetic type (Fig. 7b). The value of μ_{eff} (χT) for compound **II** at 300 K is 2.12 μ_B (0.56 cm^3 K mol^{-1}). The value obtained is noticeably lower than the theoretical value for two interacting Cu^{2+} ions: μ_{theor} = 2.44 μ_B ($\chi_{theor}T$ = 2.02 cm^3 K mol^{-1}) [24]. A similar deviation is explained by fairly strong interactions of the antiferromagnetic character. As the temperature decreases to 2 K, μ_{eff} (χT) decreases to 0.17 μ_B (0.003 cm^3 K mol^{-1}). In order to determine the exchange interaction, we approximated the experimental data on $\chi T(T)$ in the whole temperature range

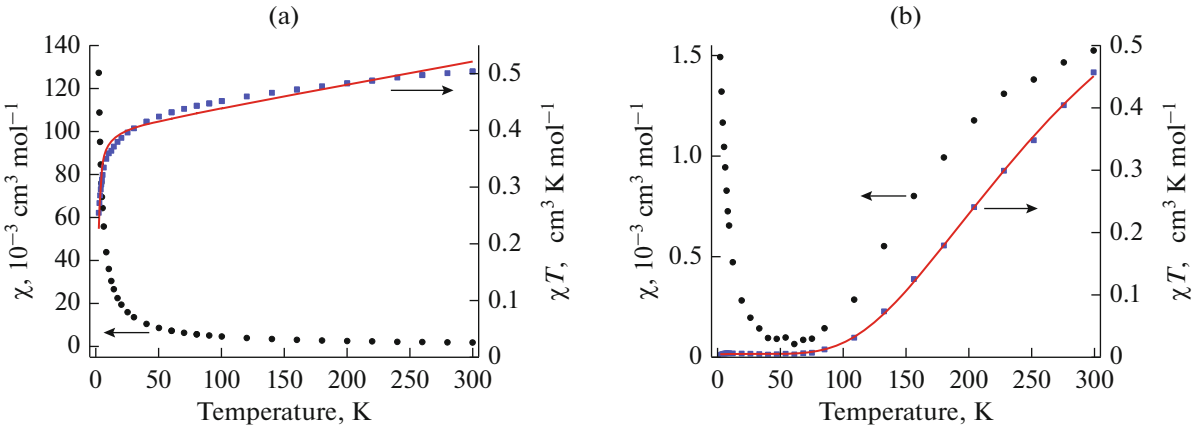

Fig. 7. Temperature dependences (○) χ and (□) χ*T* of compounds (a) **I** and (b) **II**. Lines are theoretical curves.

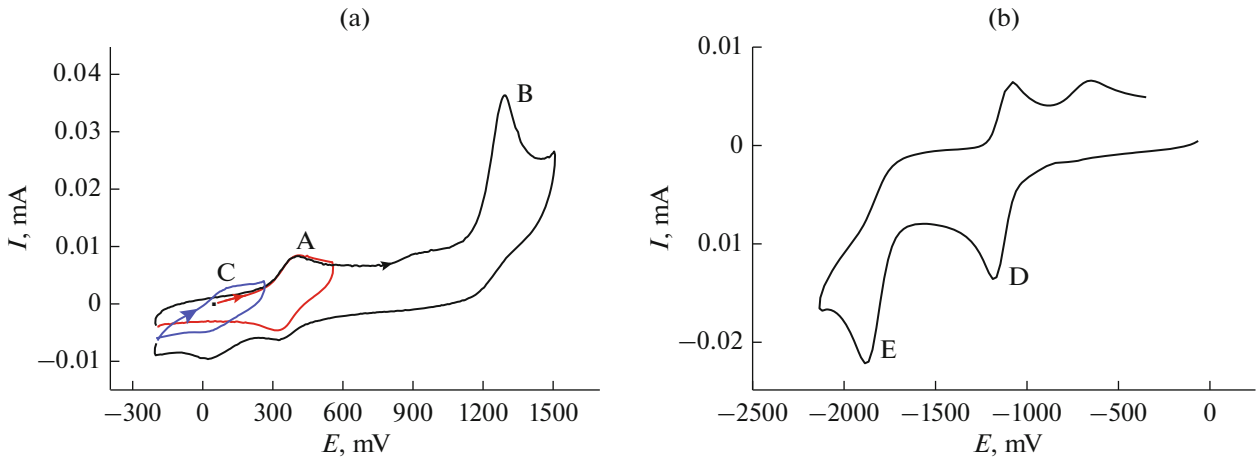

Fig. 8. CV curves observed for the (a) oxidation and (b) reduction of compound **I** vs. Ag/AgCl/KCl (0.05 M Bu_4NBF_4, DMF, 100 mV/s, Pt).

by the van Vleck equation for the case $S_1 = S_2 = 1/2$ taking into account the noninteracting paramagnetic Cu^{2+} ions.

The best fit parameters of the theoretical dependences to the experimental data ($g = 2.33 \pm 0.01$, $J = -189.0 \pm 3$ cm^{-1}) are consistent with the literature data for similar binuclear complexes [54]. The fraction of the noninteracting paramagnetic centers does not exceed 1%.

The electrochemical study of complex **I** turned out to be very informative concerning the choice between the relative contributions of two structures presented in Scheme 3. The CV study of complex **I** was carried out in DMF against 0.05 M Bu_4NBF_4. The obtained voltammetric curves are shown in Fig. 8.

Two peaks can be observed in the anodic potential region (Fig. 8a). The first peak (A) is quasi-reversible and corresponds to the one-electron oxidation process. It is most likely that the reversible transition $Cu^{2+/3+}$ occurs at this potential without changes in the structure of the coordination environment. The second peak (B) is irreversible and corresponds to the two-electron oxidation of a complex formed after the transfer of the first electron. An increase in the potential sweep to 1 V/s does not result in the appearance of a reverse peak in the CV curve, which indicates that the electron transfer is accompanied by the fast chemical step. Possible transformations that occur in the course of the electrooxidation of compound **I** are presented in Scheme 4.

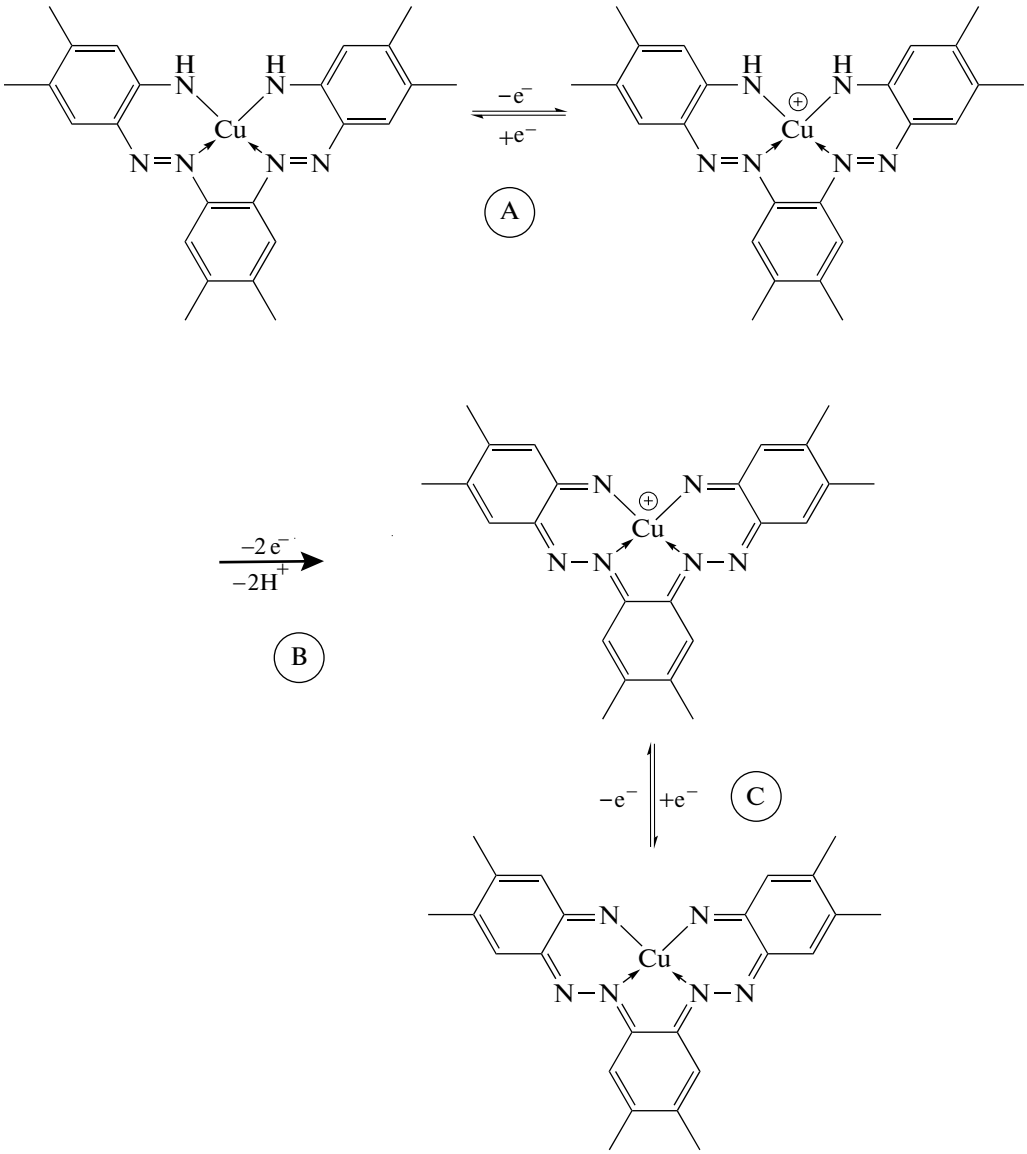

Scheme 4.

The further oxidation of the monocationic Cu(III) complex proceeds at the ligand and is accompanied by deprotonation to form a very stable bis(imino)-*ortho*-quinoid structure. This is indicated by the appearance of a new reversible redox pair (C) with $E_{1/2}$ = 52 mV, which was not observed for the initial scanning in the anodic potential region.

If the complex discussed is described by the hypothetical biradical structure [$CuL^{azo\text{-}ibsq}$] (**Ia**) presented in Scheme 3 (or the relative contribution of this form would be rather substantial), a very easy oxidation at the potentials near zero (vs. Ag/AgCl/KCl) characteristic of the Cu^0 complexes could be expected. However, this is not observed: the complex is oxidized at fairly high anodic potentials typical of the redox transition $Cu^{2+/3+}$. Thus, quinoid benzosemiquinonediimine structure **Ia** is formed only due to the deep oxidation of the complex.

Two peaks are observed in the cathodic region of the CV curve (Fig. 8b). The first peak (D) corresponds to the reversible one-electron reduction, and both the copper ion (transition $Cu^{2+/+}$) and ligand can substantially contribute to the LUMO (lowest unoccupied molecular orbital) of the complex. However, the transition of the second electron is accompanied by structure reorganization, which is distinctly seen from the irreversible character of redox transition E (Scheme 5). The potential of redox transition E is close to the reduction potential of azobenzene (−1.3 V vs. Ag/AgCl/KCl [55]). This indicates that the structure formed upon reduction is most adequately described as the Cu(II) complex with the dianionic ligand. Possible transformations that occur upon the electroreduction of compound **I** are shown in Scheme 5.

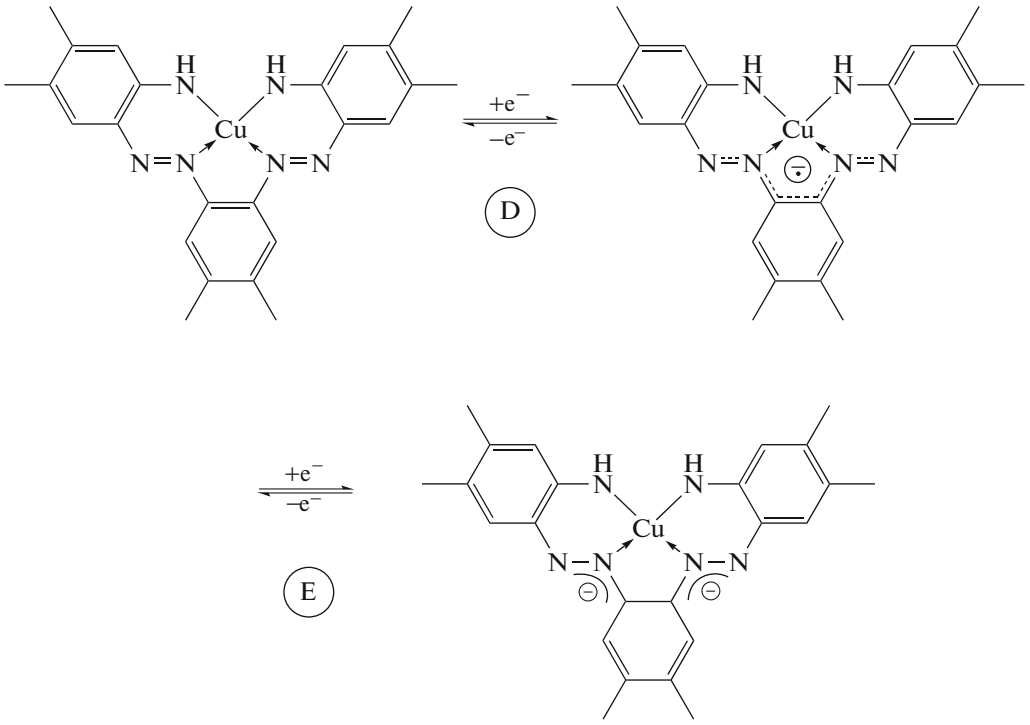

Scheme 5.

No destruction of the complex with Cu^0 formation is observed, which is indicated by the absence of the characteristic adsorption peak of Cu^0 oxidation at the electrode [56]. This is an additional evidence for the fact that the negative charge in the doubly reduced form is localized on the ligand. The proposed scheme agrees with literature data. The $[CuL_2]$ complexes with 2-phenylazopyridine [57] or 2-(arylazo)pyrimidine [58] were described. The reduction of the azoimine group in the ligand was also observed in these works.

The electrochemical study of polymer complex **II** was carried out by the introduction of the studied substance into the paste carbon electrode [59], since polymer structure **II** decomposes during dissolution in DMF. The main feature of the prepared paste electrode is the use of the ionic liquid (dodecyl(tri-*tert*-butyl)phosphonyl tetrafluoroborate) as a binding component. The use of the conducting ionic liquid makes it possible to increase the relative weight fraction of the studied electroactive substance in the paste to 25% and, therefore, to enhance the currents of the redox transitions thus improving the signal to noise ratio. For comparison, the fraction of the electroactive substance is ~5%, as a rule, when such "traditional" binding components as silicone oil are used [60]. This enabled us to determine the potential of the redox transition $Cu^{2+/+}$ for this polymer complex (E = −1.29 V vs. Ag/AgCl/KCl) (Fig. 9), and the obtained value is consistent with the data for the bridged binuclear pivalate complexes with the $\{Cu_2(Piv)_4\}$ metal cage [61]. The slight differences in potentials of the redox transitions are due to the variation of the donor properties of the axial nitrogen-containing ligands.

To conclude, the one-pot synthesis of the Cu(II) complex with hard to access symmetric *bis*-azoligand was carried out by the reaction of Dmpda with the $[Cu_2(Piv)_4(HPiv)_2]$ complex. The amine form of the ligand in the $[CuL^{azo}]$ complex (**I**) was unambiguously established by a combination of X-ray structure analysis, ESR spectroscopy, SQUID magnetometry, and electrochemical and quantum chemical studies, while the bis(diiminosemiquinone) biradical redox form of the ligand is not found in this complex. The closeness of the bond lengths in the organic moiety of the molecules of compound **I** and hypothetical electromer $[CuL^{azo\text{-}ibsq}]$ (**Ia**) observed by X-ray structure analysis was unambiguously explained by the electron density redistribution caused by the presence of the azo group. In addition, the formation of the coordination polymer $[Cu_2(Piv)_4(Dmpda)]_n$ (**II**) in which the Dmpda molecules perform the bridging function in the same reaction mixture under reduced air pressure was shown. This result proves the necessity of aerobic conditions for the catalytic transformations to occur and lead to the formation of complex **I**, which is completely consistent with the data of previous studies in the area of the aerobic copper-catalyzed organic reactions [62, 63].

ACKNOWLEDGMENTS

The X-ray structure analysis, elemental analysis, and ESR spectroscopy of the obtained compounds

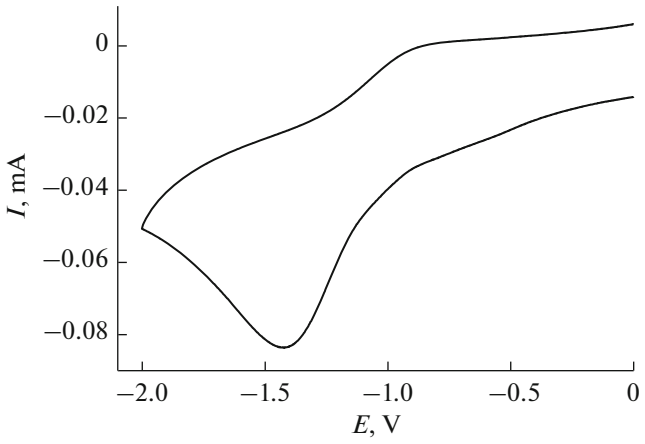

Fig. 9. Reduction of coordination polymer **II** vs. Ag/AgCl/KCl in the paste electrode composition (0.05 M Bu_4NBF_4, CH_3CN, 50 mV/s).

and the magnetochemical measurements for compound **II** were performed at the User Facilities Center of IGIC RAS within the State Assignment on Fundamental Research to the Kurnakov Institute of General and Inorganic Chemistry (Russian Academy of Sciences).

This work was supported by the Russian Science Foundation, project no. 14-23-00176.

REFERENCES

1. Balch, A.L. and Holm, R.H., *J. Am. Chem. Soc.*, 1966, vol. 88, p. 5201.
2. Eremenko, I.L., Nefedov, S.E., Sidorov, A.A., et al., *J. Organomet. Chem.*, 1998, vol. 551, p. 171.
3. Sidorov, A.A., Danilov, P.V., Nefedov, S.E., et al., *Russ. J. Inorg. Chem.*, 1998, vol. 43, p. 846.
4. Fomina, I.G., Talismanov, S.S., Sidorov, A.A., et al., *Russ. Chem. Bull.*, 2001, vol. 50, p. 515.
5. Herebian, D., Bothe, E., Neese, F., et al., *J. Am. Chem. Soc.*, 2003, vol. 125, p. 9116.
6. Khusniyarov, M.M., Harms, K., Burghaus, O., et al., *Dalton Trans.*, 2008, p. 1355.
7. Stokes, F.A., Kloo, L., Lv, Y., et al., *Chem. Commun.*, 2012, vol. 48, p. 11298.
8. Mederos, A., Dominguez, S., Hernandez-Molina, R., et al., *Coord. Chem. Rev.*, 1999, vols. 193–195, p. 913.
9. Poddel'sky, A.I., Cherkasov, V.K., and Abakumov, G.A., *Coord. Chem. Rev.*, 2009, vol. 253, p. 291.
10. Olivos Suarez, A.I., Lyaskovskyy, V., Reek, J.N.H., et al., *Angew. Chem., Int. Ed. Engl.*, 2013, vol. 52, p. 12510.
11. Sidorov, A.A., Fomina, I.G., Nesterov, V.V., et al., *Russ. Chem. Bull.*, 1999, vol. 48, no. 3, p. 573.
12. Leconte, N., Ciccione, J., Gellon, G., et al., *Chem. Commun.*, 2014, vol. 50, p. 1918.
13. Ciccione, J., Leconte, N., Luneau, D., et al., *Inorg. Chem.*, 2016, vol. 55, p. 649.
14. Talismanova, M.O., Fomina, I.G., Sidorov, A.A., et al., *Russ. Chem. Bull.*, 2003, vol. 52, no. 12, p. 2706.
15. Fomina, I.G., Sidorov, A.A., Aleksandrov, G.G., et al., *Russ. Chem. Bull.,* 2002, vol. 51, no. 8, p. 1581.
16. Malkov, A.E., Aleksandrov, G.G., Ikorskii, V.N., et al., *Russ. J. Coord. Chem.*, 2001, vol. 27, no. 9, p. 636.
17. Malkov, A.E., Sidorov, A.A., Aleksandrov, G.G., et al., *Russ. Chem. Bull.,* 2003, vol. 52, no. 3, p. 710.
18. Eremenko, I.L., Malkov, A.E., Sidorov, A.A., et al., *Mendeleev Commun.*, 2003, vol. 13, no. 1, p. 10.
19. Troyanov, S.I., Il'ina, E.G., Dunaeva, K.M., *Koord. Khim.*, 1991, vol. 17, no. 12, p. 1692.
20. Denisova, T.O., Amel'chenkova, E.V., Pruss, I.V., et al., *Russ. J. Inorg. Chem.*, 2006, vol. 51, no. 7, p. 1020.
21. *SMART (control) and SAINT (integration) Software. Version 5.0*, Madison: Bruker AXS Inc., 1997.
22. Sheldrick, G.M., *SADABS. Program for Scanning and Correction of Area Detector Data*, Göttinngen: Univ. of Göttinngen, 2004.
23. Sheldrick, G.M., *Acta Crystallogr., Sect. A: Found. Crystallogr.*, 2008, vol. 64, no. 1, p. 112.
24. Rakitin, Yu.V. and Kalinnikov, V.T., *Sovremennaya magnetokhimiya* (Modern Magnetochemistry), St. Petersburg: Nauka, 1994.
25. Frisch, M.J., Trucks, G.W., Schlegel, H.B., et al., *Gaussian 09 (revision E.01)*, Wallingford: Gaussian, Inc., 2013.
26. Starikov, A.G., Minyaev, R.M., and Minkin, V.I., *J. Mol. Struct.: THEOCHEM*, 2009, vol. 895, nos. 1–3, p. 138.
27. Chemcraft. Version 1.7. 2013. http://www.chemcraft-prog.com.
28. Reuter, R., Hostettler, N., Neuburger, M., and Wegner, H.A., *Eur. J. Org. Chem.*, 2009, vol. 2009, p. 5647.
29. Hamon, F., Djedaini-Pilard, F., Barbot, F., and Len, C., *Tetrahedron*, 2009, vol. 65, p. 10105.
30. Bellotto, S., Reuter, R., Heinis, C., and Wegner, H.A., *Org. Chem.*, 2011, vol. 76, p. 9826.
31. Kang, H.-M., Kim, H.-Y., Jung, J.-W., and Cho, C.G., *J. Org. Chem.*, 2007, vol. 72, p. 679.
32. Mathews, M. and Tamaoki, N., *J. Am. Chem. Soc.*, 2008, vol. 130, p. 11409.
33. Takaishi, K., Kawamoto, M., Muranaka, A., and Uchiyama, M., *Org. Lett.*, 2012, vol. 14, no. 13, p. 3252.
34. Kerner, L., Kickova, A., Filo, J., et al., *J. Phys. Chem. A*, 2015, vol. 119, p. 8588.
35. Lu, J., Xia, A., Zhou, N., et al., *Chem.-Eur. J.*, 2015, vol. 21, p. 2324.
36. Allen, F.H., Kennard, O., Watson, D.G., et al., *Perkin Trans. II.*, 1987, p. S1.
37. Adams, H., Bucknall, R.M., Fenton, D.E., et al., *Polyhedron*, 1998, vol. 17, nos. 23–24, p. 4169.
38. Dhara, P.K., Pramanik, S., Lu, T.-H., et al., *Polyhedron*, 2004, vol. 23, p. 2457.
39. Jarvis, J.A.J., *Acta Crystallogr.*, 1961, vol. 14, no. 9, p. 961.
40. Benaouida, M.A., Benosmane, A., Bouguerria, H., et al., *Acta Crystallogr., Sect. E*: *Struct. Rep. Online*, 2013, vol. 69, p. m405.

41. Abrahams, B.F., Egan, S.J., and Robson, R., *J. Am. Chem. Soc.*, 1999, vol. 121, no. 14, p. 3535.

42. Sarkar, S., Dhara, P.K., Nethaji, M., and Chattopadhyay, P., *J. Coord. Chem.*, 2009, vol. 62, no. 5, p. 817.

43. Tai, W.-J., Li, C.-H., Li, C.-Y., and Ko, B.-T., *Acta Crystallogr., Sect. E*: *Struct. Rep. Online*, 2010, vol. 66, p. m1315.

44. Burlov, A.S., Uraev, A.I., Lyssenko, K.A., et al., *Russ. J. Coord. Chem.*, 2006, vol. 32, no. 9, p. 686. doi 10.1134/S1070328406090119

45. Speier, G., Csihony, J., Whalen, A.M., and Pierpont, C.G., *Inorg. Chem.*, 1996, vol. 35, p. 3519.

46. Burlov, A.S., Uraev, A.I., Matuev, P.V., et al., *Russ. J. Coord. Chem.*, 2008, vol. 34, no. 12, p. 904. doi 10.1134/S1070328408120063

47. Bill, E., Bothe, E., Chaudhuri, P., et al., *Chem.-Eur. J.*, 2005, vol. 11, p. 204.

48. Ng, S.W., *Acta Crystallogr., Sect. E*: *Struct. Rep. Online*, 2009, vol. 65, p. o1069.

49. Stibrany, R.T. and Potenza, J.A., *CSD Commun.*, 2012 (Private Communication; refcode GOGWEG, CCDC 893911).

50. Rakitin, Yu.V., Larin, G.M., and Minin, V.V. *Interpretatsiya spektrov EPR koordinatsionnykh soedinenii* (Interpretation of the ESR Spectra of Coordination Compounds), Moscow: Nauka, 1993.

51. Lebedev, Ya.S. and Muromtsev, V.I., *EPR i relaksatsiya stabilizirovannykh radikalov* (ESR and Relaxation of Stabilized Radicals), Moscow: Khimiya, 1972, p. 25.

52. Wilson, R. and Kivelson, D., *J. Chem. Phys.*, 1966, vol. 44, no. 1, p. 154.

53. Belford, G.G., Belford, R.L., and Burkhalter, J.F., *J. Magn. Reson.*, 1973, vol. 11, no. 2, p. 251.

54. Yakovenko, A.V., Kolotilov, S.V., Cador, O., et al., *Eur. J. Inorg. Chem.*, 2009, no. 16, p. 2354.

55. Utley, J.H.P. and Nielsen, M.F., *Organic Electrochemistry*, Lund, H. and Hammerich, O., N.Y., Eds., Marcel Dekker, Inc., 2001, p. 1227.

56. McCann, M., Cronin, J.F., Devereux, M., et al., *Polyhedron*, 1995, vol. 14, nos. 23–24, p. 3617.

57. Datta, D. and Chakravorty, A., *Inorg. Chem.*, 1983, vol. 22, no. 7, p. 1085.

58. Santra, P.K., Das, D., Misra, T.K., et al., *Polyhedron*, 1999, vol. 18, no. 14, p. 1909.

59. McCreery, R.L., *Chem. Rev.*, 2008, vol. 108, no. 7, p. 2646.

60. Khrizanforov, M.N., Arkhipova, D.M., Shekurov, R.P., et al., *J. Solid State Electrochem.*, 2015, vol. 19, no. 9, p. 2883.

61. Fomina, I., Dobrokhotova, Zh., Aleksandrov, G., et al., *Polyhedron*, 2010, vol. 29, no. 7, p. 1734.

62. Zhang, C. and Jiao, N., *Angew. Chem., Int. Ed.*, 2010, vol. 49, no. 35, p. 6174.

63. Allen, S.E., Walvoord, R.R., Padilla-Salinas, R., and Kozlowski, M.C., *Chem. Rev.*, 2013, vol. 113, no. 8, p. 6234.

Translated by E. Yablonskaya